

## Aggregation and Tautomeric Properties of CI Acid Red 138

T. Iijima,<sup>a</sup> E. Jojima,<sup>a</sup> L. Antonov,<sup>b</sup> St. Stoyanov<sup>c</sup> & T. Stoyanova<sup>c</sup>

<sup>a</sup>Department of Textile Science, Jissen Women's University, Hino 4-1-1, Tokyo, Japan

<sup>b</sup>Department of Ecology, National Forestry University, Sofia 1756, Bulgaria

<sup>c</sup>Department of Chemistry, University of Sofia, Sofia 1164, Bulgaria

(Received 4 March 1997; accepted 14 April 1997)

### ABSTRACT

*The spectral properties of CI Acid Red 138 and related dyes in respect of their azo(A)-hydrazone(H) tautomeric behavior were investigated. The observed influence of temperature and concentration was taken into account in the described theoretical model. The absorption spectra of the H-form and its corresponding H-dimer were calculated along with the structural parameters—the distance R between the molecules in the dimer ( $\sim 5.3$  Å) and the angle  $\alpha$  between the transition dipole moments ( $\sim 56^\circ$ ). © 1998 Elsevier Science Ltd*

**Keywords:** CI Acid Red 138, tautomeric properties.

### INTRODUCTION

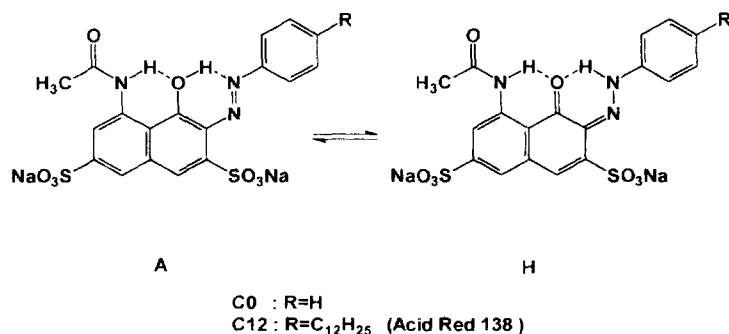
The azo dye CI Acid Red 138 (C12) and its homologues belong to the group of 2-phenylazo-1-naphthols, where two tautomeric structures are possible [1], viz. azo (A) and hydrazone (H) (Scheme 1).

For this reason, in many cases the interaction of the dye with its environment, e.g. solvent [2], dye [3, 4], macromolecule [5], and other additives such as cyclodextrins [6, 7], leads to change of the absorption spectra. Based on the spectral changes, the mechanism of these interactions can be discussed.

The aim of this study is to investigate in more detail the aggregation and tautomeric phenomena of C12 in order to elucidate their mutual dependence, influencing the spectral properties of this practically important dye.

### EXPERIMENTAL

The spectral properties of C12 were investigated as a function of the temperature and concentration. The UV–Vis absorption spectra were recorded



Scheme 1

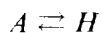
in distilled water using a Shimadzu MPS-2000 spectrophotometer at four different temperatures (25, 35, 45 and 55°C) and at different dye concentrations, keeping the value of  $C_0l$  constant ( $C_0l = 7.512 \times 10^{-5}\text{M}$ ). The spectral data obtained were processed according to the theoretical model described next.

## THEORETICAL MODEL

The measured experimental data ( $A_{i,j}$ ) at a definite wavelength can be presented as a function of the different temperatures ( $T_j$ ) and dye concentrations ( $C_0^i$ ), where  $i$  is the solution index ( $i = 1 \div m$ ;  $m$  is number of the concentrations used) and  $j$  is the temperature index ( $j = 1 \div n$ ;  $n$  is number of the temperatures applied). The model can be described as follows.

### Equilibria and constants

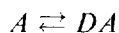
(a) Azo(A)-hydrazone(H) tautomerism



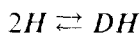
$$K_T^j = C_A^{i,j} / C_H^{i,j} \quad (1)$$

where  $K_T^j$  is the tautomeric constant at  $j$ th temperature;  $C_A^{i,j}$  and  $C_H^{i,j}$  are the concentrations of A and H-form, respectively, at  $j$ th temperature in  $i$ th solution.

(b) Dimerization of both A- and H-tautomers



$$K_{DA}^j = \frac{C_{DA}^{i,j}}{(C_A^{i,j})^2} \quad (2)$$



$$K_{DH}^j = \frac{C_{DH}^{i,j}}{(C_H^{i,j})^2} \quad (3)$$

where  $K_{DA}^j$  and  $K_{DH}^j$  are the aggregation constants of A- and H-forms at the  $j$ th temperature;  $C_{DA}^{i,j}$  and  $C_{DH}^{i,j}$  are the concentrations of the A-dimer (DA) and H-dimer (DH) at the  $j$ th temperature in the  $i$ th solution.

### Mass balance

$$C_H^{i,j} + C_A^{i,j} + 2C_{DA}^{i,j} + 2C_{DH}^{i,j} = C_0^i \quad (4)$$

### Additivity principle

$$A_{i,j} = l^i \cdot \left\{ C_H^{i,j} \cdot \varepsilon_H + C_A^{i,j} \cdot \varepsilon_A + C_{DH}^{i,j} \cdot \varepsilon_{DH} + C_{DA}^{i,j} \cdot \varepsilon_{DA} \right\} \quad (5)$$

where  $l^i$  is the path length of the  $i$ th solution;  $\varepsilon_H$ ,  $\varepsilon_A$ ,  $\varepsilon_{DH}$  and  $\varepsilon_{DA}$  are individual molar absorptivities of the fourth forms in the system.

Using the denotations of eqns (6)–(9)

$$X_H^{i,j} = \frac{C_H^{i,j}}{C_0^i} \quad (6)$$

$$X_A^{i,j} = \frac{C_A^{i,j}}{C_0^i} \quad (7)$$

$$X_{DH}^{i,j} = \frac{C_{DH}^{i,j}}{C_0^i} \quad (8)$$

$$X_{DA}^{i,j} = \frac{C_{DA}^{i,j}}{C_0^i} \quad (9)$$

eqns (1)–(5) can be written as follows:

$$K_T^j = \frac{X_A^{i,j}}{X_H^{i,j}} \quad (10)$$

$$K_{DA}^j = \frac{X_{DA}^{i,j}}{2C_0^i (X_A^{i,j})^2} \quad (11)$$

$$K_{DH}^j = \frac{X_{DH}^{ij}}{2C_0^i (X_H^{ij})^2} \quad (12)$$

$$X_H^{ij} + X_A^{ij} + X_{DH}^{ij} + X_{DA}^{ij} = 1 \quad (13)$$

$$A_{ij} = X_H^{ij} \cdot A_H + X_A^{ij} \cdot A_A + X_{DH}^{ij} \cdot A_{DH} + X_{DA}^{ij} \cdot A_{DH} \quad (14)$$

where  $X$  is the mole fraction.

$$\begin{aligned} A_H &= \varepsilon_H \cdot C_0^i \cdot l^i \\ A_A &= \varepsilon_A \cdot C_0^i \cdot l^i \\ A_{DH} &= \varepsilon_{DH} \cdot C_0^i \cdot l^i / 2 \\ A_{DA} &= \varepsilon_{DA} \cdot C_0^i \cdot l^i / 2 \end{aligned}$$

After simple mathematical transformations, eqn (13) can be presented as a function on  $X_H$  only:

$$X_H^{ij} \cdot (1 + K_T^j) + (X_H^{ij})^2 \cdot 2C_0^i \cdot (K_{DH}^j + (K_T^j)^2 \cdot K_{DA}^j) = 1 \quad (15)$$

so that:

$$X_H^{ij} = \frac{-(1 + K_T^j) + \sqrt{(1 + K_T^j)^2 + 8C_0^i \cdot (K_{DH}^j + (K_T^j)^2 \cdot K_{DA}^j)}}{4C_0^i (K_{DH}^j + (K_T^j)^2 \cdot K_{DA}^j)} \quad (16)$$

In contrast,

$$A_{ij} = X_H^{ij} \cdot (A_H + K_T^j A_A) + 2C_0^i (X_H^{ij})^2 \cdot (A_{DH} K_{DH}^j + A_{DA} K_{DA}^j (K_T^j)^2) \quad (17)$$

Equations (16) and (17) describe an optimization function, depending on  $K_T^j$ ,  $K_{DH}^j$ ,  $K_{DA}^j$ ,  $A_A$ ,  $A_H$ ,  $A_{DA}$  and  $A_{DH}$  (totally  $3n+4$  parameters) and determined by  $n \cdot m$  experimental points ( $A_{ij}$ ).

## RESULTS AND DISCUSSION

The absorption spectra of c12 at different concentrations (25°C) are presented in Fig. 1.

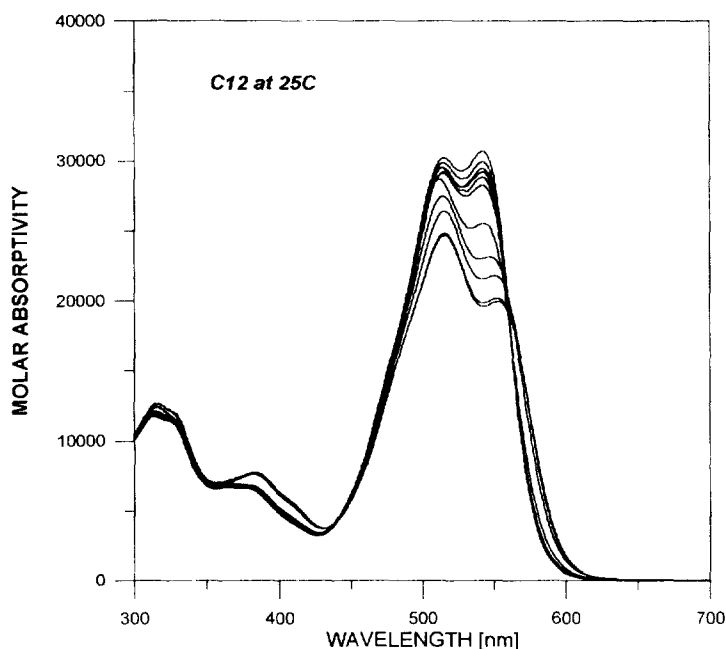


**Fig. 1.** Absorption spectra of c12 in a range of different concentrations, from  $7.51 \times 10^{-4}$  M to  $5.14 \times 10^{-6}$  M, keeping the value  $C_0 I^0 = \text{const} = 7.51 \times 10^{-5}$  M.

The increase of  $C_0$  leads to a decrease of the intensity of the absorption maxima at 500 nm and  $\sim 540$  nm and appearance of a poorly defined shoulder at  $\sim 580$  nm. The observed isosbestic point at  $\sim 560$  nm suggests the existence of monomer–dimer equilibrium, most probably  $H \rightleftharpoons DH$ , according to our previous data, showing that in dye c12 the H-form is strongly predominating [1].

Additional support for the existence of monomer–dimer equilibrium comes from the absorption spectra of c12 in *n*-butanol/*i*-octane mixtures (Fig. 2). In the most hydrophobic environment, i.e. *n*-butanol/*i*-octane 20:80, spectral changes similar to those in Fig. 1 are observed.

In our previous study [1] we have suggested another principal possibility for an explanation of the observed spectral changes in Fig. 2. Concerning the observed shape of the long wavelength absorption band, the intensities of the discrete vibronic transitions depend on the overall equilibrium geometry difference between the ground and first excited singlet states of c12. When particular chemical interactions between a dye molecule and its environment occur, e.g. specific solvation or aggregation effects, they could change the equilibrium geometry of the  $S_0$  and  $S_1$  states, and a change in the relative intensities of the discrete vibronic bands within the long wavelength absorption band may occur. However, although the H-form is dominant, the

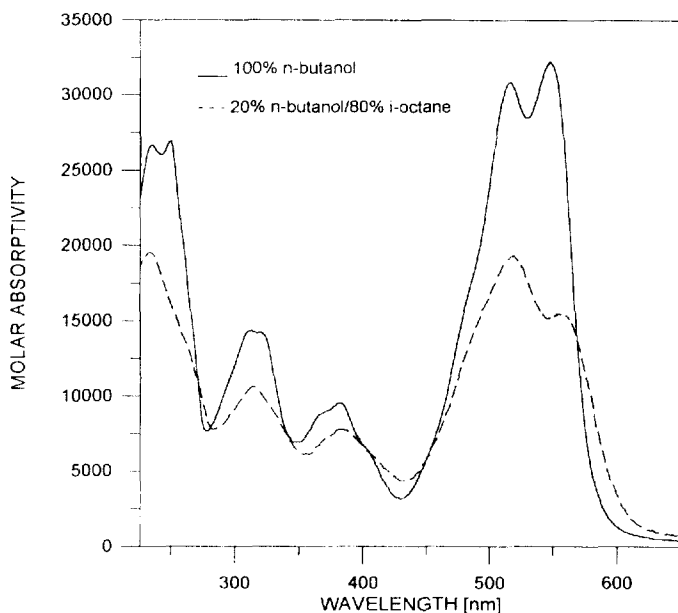


Fig. 2. Absorption spectra of c12 in *n*-butanol and *i*-octane/*n*-butanol 80:20,  $C_0 = 2.12 \times 10^{-5}$  M.

existence of the A-form cannot be excluded. In the second derivative spectra for the most diluted and concentrated solutions of c12 (Fig. 3), a peak at about 460–470 nm is observed, which could be assigned to the A-form.

This peak is also clearly observed in the polarized absorption spectra of c12 in a drawn PVA film (Fig. 4) [8]. It could be expected that in the PVA matrix the orientation of c12 on drawing depends on the value of the ground

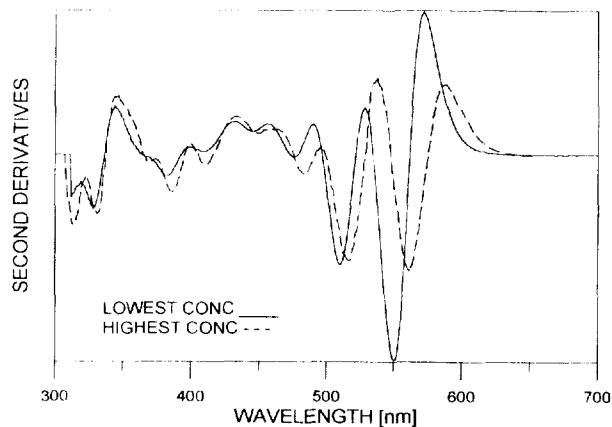
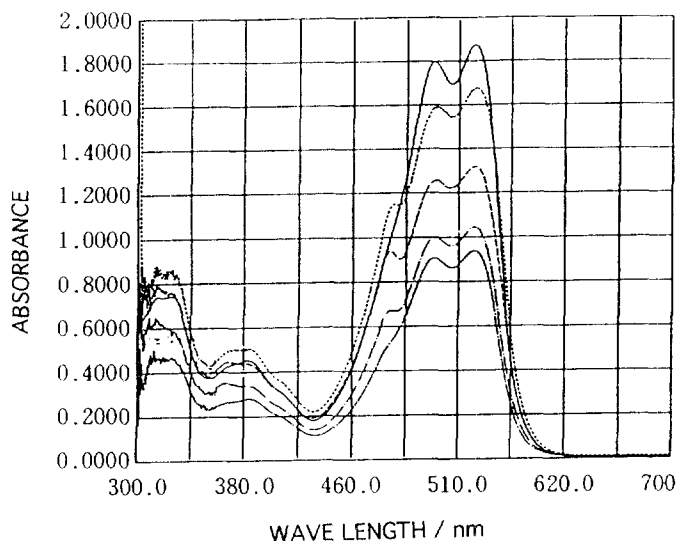


Fig. 3. Second derivative spectra of the most diluted and concentrated solutions of c12 from Fig. 1.



**Fig. 4.** Polarized absorption spectra of CI2 in drawn PVA film matrix (draw ratio 3.0) in decreasing order of absorbance values; undrawn 0°, 0°, 30°, 60° and 90° polarization angles.

state dipole moments, while the intensity of the long wavelength absorption band depends on the extent of interaction between the polarized incident light and the directions of the transition dipole moments for both the A- and H-tautomeric forms.

The calculated, within the PPP-MO approximation [1, 9], ground state dipole moments ( $\mu_{S0}$ ), the transition dipole moments ( $TM$ ) for A- and H-forms and their corresponding angles ( $\alpha$ ), calculated according to eqns (18) and (19) for the parent dye C0, are collected in Table 1.

$$\operatorname{tg} \alpha = \mu_{S0}^y / \mu_{S0}^x \quad (18)$$

$$\operatorname{tg} \alpha = TM^y / TM^x \quad (19)$$

where  $x$  and  $y$  denote the components of the dipole moments.

**TABLE 1**  
Ground State and Transition Dipole Moments for Tautomeric A- and H-Forms of C0.

Calculated value	A-form	H-form
$\mu_{S0}$	0.51	3.14
$TM$	1.67	2.18
$\alpha^\circ(\mu_{S0})$	2°	-30°
$\alpha^\circ(TM)$	-14°	23°

It might be expected that the different directions of the ground state dipole moments for A- and H-forms will lead to a different orientation of these tautomeric forms within the drawn PVA films, and consequently to a different extent of interaction with the incident polarized light. As a result the absorption band at approximately 470 nm, assigned for the A-form, appears distinctly in the polarization absorption spectra of c12 (Fig. 4). It should be noted also that the difference between the directions of the transition dipole moments (TM) and the ground state dipole moments ( $\mu_{S_0}$ ), i.e.  $\alpha_{TM}-\alpha_{\mu_{S_0}}$ , could be connected with the observed maximal intensity of the polarized absorption long wavelength maximum at about 150–160° in the drawn PVA film (Fig. 5) [8].)

However, the absorption spectra of the most diluted solution at different temperatures, shown in Fig. 6 exhibit a decrease of the H-band's intensities at 500 and 540 nm and suggest that the observed spectral changes are not due to  $H \rightleftharpoons DH$  equilibrium, since the increase of the temperature leads generally to disaggregation [10] and an increase of these bands should be expected. The decrease of H-band's intensity might be connected with  $A \rightleftharpoons H$  tautomeric equilibrium, shifted towards the A-form with the increase of the temperature [11].

For the reasons discussed above, in the solutions investigated at different  $T$  and concentration, a kind of mixed equilibrium between A, H, DH, and DA could be expected.

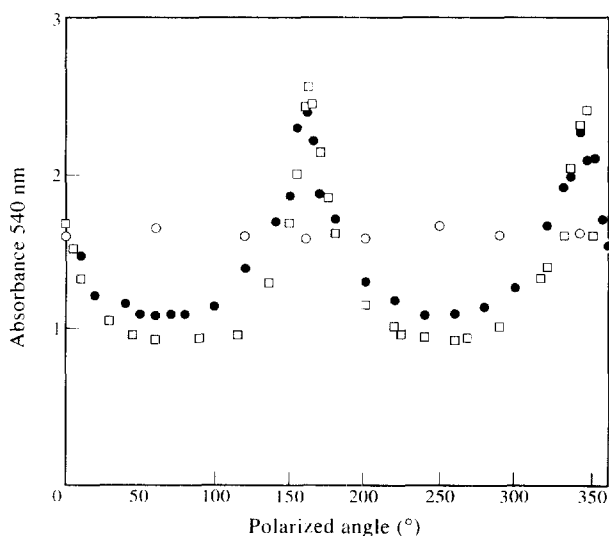


Fig. 5. Polarized angle dependence of absorbance for c12 in PVA film with the draw ratio: ○, undrawn; ●, 2.0; □, 3.0.



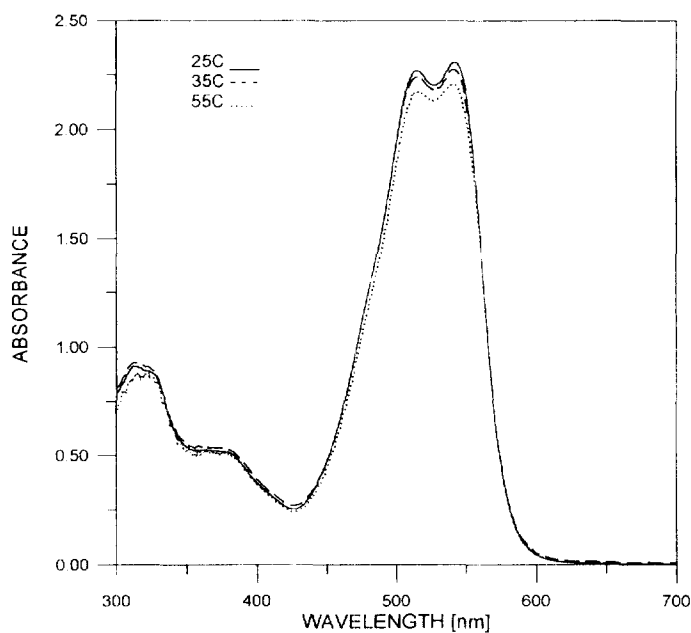


Fig. 6. Absorption spectra of c12 at different temperatures ( $C_0 = 5.14 \times 10^{-6}$  M).

TABLE 2  
Calculated Values of the Equilibrium Constants at Different  $T$

$T$	$K_T$	$K_{DH}$	$K_{DA}$
23°	0.184	642	89.9
35°	0.251	415	14.6
45°	0.314	328	2.7
55°	0.425	262	1.2

Applying the described theoretical model (eqn (17)) at 542 nm, where the sensitivity of the observed spectral changes is the highest, the values of equilibrium constants were obtained (Table 2). In all cases the H-form is predominating and the DA form can practically be neglected. The optimization results without DA in the model are essentially the same.

Increase of  $T$  leads to an increase of the A-form and to a rapid decrease in the concentrations of both dimers. Using the well known equations, connecting the values of  $\ln K$  with  $T$ , [7], the thermodynamic parameters of the tautomeric and monomer-dimer equilibria were evaluated. The results for the enthalpy ( $\Delta H$ ) and entropy ( $\Delta S$ ) terms are presented in Table 3. Evidently the contribution of the entropy part is predominant.

The absorption spectra of the H and DH forms, calculated according to eqn (17), are presented in Fig. 7. The dimer spectrum shows two bands

**TABLE 3**  
Evaluated Thermodynamic Parameters of the Investigated Processes

Equilibrium processes	$\Delta H$ (kJ mol <sup>-1</sup> )	$\Delta S$ (kJ mol <sup>-1</sup> K <sup>-1</sup> )
$H \rightleftharpoons A$	22.24	60.59
$2A \rightleftharpoons DA$	-118.12	-360.48
$2H \rightleftharpoons DH$	-26.15	-23.67

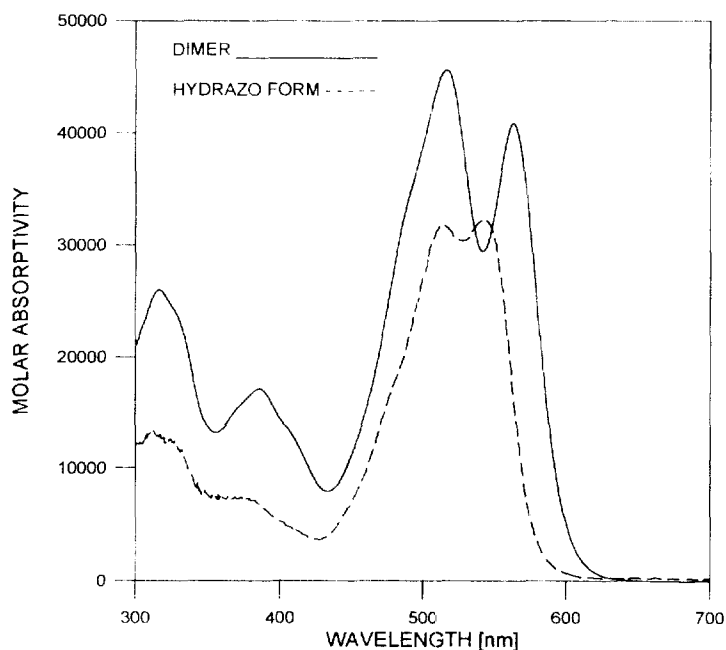


**Fig. 7.** Calculated individual absorption spectra of the H- and H-dimer (DH) forms.

slightly shifted in respect to the monomer ones—a long wavelength J-band and a short wavelength H-band [12].

The structural characteristics of the hydrazone dimer were calculated according to eqns (20) and (21) [12] and the data are collected in Table 4.

$$\alpha = 2 \cdot \arctg \cdot \left\{ \frac{\nu_H \cdot f_J}{\nu_J \cdot f_H} \right\}^{\frac{1}{2}} \quad (20)$$

$$R = \left\{ \frac{2.14 \times 10^{10} \cdot \cos \alpha \cdot f_M}{\nu_M \cdot \Delta \nu} \right\} \quad (21)$$

**TABLE 4**  
Spectral Characteristics of the Monomer and Dimer Bands

Band	$\nu(\text{cm}^{-1})$	$f$
M—	18,415	0.48
H—	19,810	0.55
J—	17,665	0.14

where  $\nu_H$  and  $\nu_J$  are the absorption maxima of H- and J-bands respectively in  $\text{cm}^{-1}$ ;  $f_M$ ,  $f_H$  and  $f_J$  are the corresponding oscillator strengths;  $\Delta\nu = \nu_H - \nu_J$ ;  $\alpha$  is the angle between the transition dipole moments of monomeric molecules within the dimer and  $R$  is the distance between the two adjacent molecules in the dimer.

The calculated angle  $\alpha$  and the distance  $R$  were estimated to about  $\sim 56^\circ$  and 5.3 Å. Since the molar part of the A-form and especially the DA-form are very small (Table 2), the calculating error of their individual spectra is too high, and this does not allow the spectra and structural parameters of these forms to be correctly estimated.

## CONCLUSION

The absorption properties and color of the potentially tautomeric azo dye CI Acid Red 138 depend not only on the position of the tautomeric azo-hydrazone equilibrium, but also on the environment of the molecule (solvent or polymer matrix), temperature and concentration. In such dyes all these factors should be considered in order to elucidate the relationship between the structure and spectral properties.

## ACKNOWLEDGEMENTS

Financial support from the National Science Foundation (project X-471) is gratefully acknowledged by L.A., S.S. and T.S.

## REFERENCES

1. Stoyanov, St., Iijima, T., Stoyanova, T. and Antonov, L., *Dyes and Pigments*, 1995, **27**, 237.
2. Zollinger, H., *Colour Chemistry*, 2nd revised edn. VCH, New York, 1991, **413** pp. 24.
3. Karube, Y. and Iijima, T., *Sen-i Gakkaishi*, 1992, **48**, 481.
4. Kobayashi, Y., Tanizaki, Y. and Ando, N., *Bull. Chem. Soc. Jpn*, 1960, **33**, 61.

5. Nakano, Y., Seki, T., Wata, H., Komiyama, J. and Iijima, T., *Colloid Polymer Sci.*, 1982, **260**, 218.
6. Hersey, A. and Robinson, B. H., *J. Chem. Soc. Faraday Trans. I*, 1984, **80**, 2039.
7. Karube, Y. and Iijima, T., *Sen-i Gakkaishi*, 1994, **50**, 477, and references cited therein.
8. Iijima, T. and Jojima, E., *Bull. Fac. Environm. Sci., Jissen Women's Univ.*, 1996, **33**, 45.
9. Griffiths, J., *Dyes and Pigments*, 1982, **3**, 211.
10. Stoyanov, St., Deligeorgiev, T. and Simov, D., *J. Mol. Struct.*, 1984, **115**, 363 and references cited therein.
11. Stoyanov, St. and Antonov, L., *Dyes and Pigments*, 1983, **10**, 33.
12. Kasha, M., Rawls, H. R. and El-Bayoumi, M. A., *Pure Appl. Chem.*, 1965, **11**, 371.